



Maximum late Holocene extent of the western Greenland Ice Sheet during the late 20th century

Samuel E. Kelley*, Jason P. Briner, Nicolás E. Young¹, Gregory S. Babonis, Bea Csatho

Department of Geology, University at Buffalo, Buffalo, NY 14260, USA

ARTICLE INFO

Article history:

Received 27 June 2012

Received in revised form

14 September 2012

Accepted 17 September 2012

Available online

Keywords:

Greenland Ice Sheet

Little Ice Age

¹⁰Be exposure dating

Ice-dammed lake

Lake sediment core

ABSTRACT

The pattern of Greenland Ice Sheet margin change during the 20th century is variable. Large-scale retreat of marine-outlet glaciers contrasts with the often-negligible retreat observed along land-terminating margins of the ice sheet. We reconstruct a chronology of ice-margin change for two land-terminating ice margins in western Greenland using radiocarbon and ¹⁰Be exposure dating. Our results indicate that two land-terminating lobes attained their maximum late Holocene position in the late 20th century. This contrasts with the nearby marine-terminating Jakobshavn Isbræ, which achieved a maximum late Holocene position during the Little Ice Age, and has since retreated ca 40 km. In addition, we survey ice-margin change across western Greenland, utilizing satellite imagery. We find that many land-terminating sectors of the ice sheet, in addition to our study area, may have attained their maximum late Holocene extent during the 20th century. This suggests a lagged ice-margin response to prior cooling, such as the Little Ice Age, which would imply significant retreat of land-terminating sections of the Greenland Ice Sheet in response to 20th and 21st century warming may be yet to come.

© 2012 Elsevier Ltd. All rights reserved.

1. Introduction

Since the Little Ice Age (LIA; ca 1250–1900 AD), most glaciers worldwide have experienced net retreat (Lowell, 2000; Oerlemans, 2005). Glacier retreat has been driven by a general warming trend throughout the late 19th–21st centuries, which ended the cumulative build up of glaciers during the late Holocene (e.g., Porter, 2007). Despite local influences on glacier change such as hypsometry, internal dynamics, and variations in lag time that all glaciers have with respect to changing climate, most glaciers retreated in concert with recent warming on decadal timescales (Lowell, 2000; Oerlemans, 2005). This is best documented in alpine glacier systems, with far fewer records that gauge the response of ice sheets to climate change on decadal timescales.

Recent observations of the Greenland Ice Sheet (GIS) reveal dramatic changes in thickness and surface velocity and are leading to an improved understanding of its response to climate change (Rignot and Kanagaratnam, 2006; Van den Broeke et al., 2009; Rignot et al., 2010). First thought to be perhaps thousands of years,

it appears now that the response time of ice sheets might be much shorter (Bamber et al., 2007). This is particularly true for fast-flowing outlet glaciers, which at present have response times on the order of years to decades (Bamber et al., 2007). Indeed, in southeastern Greenland, a relatively close coupling between glacier change and air temperature from the 1930s to present has recently been documented (Bjork et al., 2012). It has also been demonstrated that the GIS is able to respond to short-lived abrupt climate events in the past (Young et al., 2011a, 2011b).

Reconstructing ice-margin fluctuations that pre-date the instrumental record can improve our understanding of the complex nature by which the GIS responds to climate change. Recent studies in eastern Disko Bugt place the timing of retreat of the ice sheet onto land ca 10 ka (Weidick and Bennike, 2007; Long et al., 2011; Young et al., 2011a) and subsequent retreat resulting in a smaller than present ice-sheet configuration by ca 7 ka (Weidick and Bennike, 2007; Briner et al., 2010; Young et al., 2011a). Ice advance occurred throughout the late Holocene (Weidick, 1992; Briner et al., 2011), although most information on the late Holocene ice advance is from marine ice-sheet sectors. Following expansion during the late Holocene, the GIS margin has largely retreated (Weidick, 1968; Rignot et al., 2008), with the most pronounced retreat occurring at large outlet glaciers such as Jakobshavn Isbræ (Joughin et al., 2004; Weidick and Bennike, 2007; Csatho et al., 2008). However, post-LIA

* Corresponding author.

E-mail address: samuelke@buffalo.edu (S.E. Kelley).

¹ Present address: Lamont-Doherty Observatory, Columbia University, New York, NY 10964, USA.

retreat has not been uniform in space and time across Greenland, with some sectors experiencing no retreat or even a net advance during the 20th century (Weidick, 1968). Here, our goal is to investigate fluctuations of the western GIS ice margin during the late Holocene in a land-terminating setting. Furthermore, we aim to place our findings into a wider context by examining the spatial pattern of ice-margin change from the late Holocene maximum to the present throughout western Greenland.

2. Materials and methods

2.1. Field investigation

We visited two adjacent valleys in southeastern Disko Bugt, located ca 60 km south of Jakobshavn Isbræ, western Greenland (Fig. 1). The Qinngap Ilulialeraa–Kuussuup Tasia (QK) and Tininnilik valleys each contain proglacial lakes with contrasting physiographies. Qinngap Ilulialeraa (160 m asl) abuts the ice

margin on the lake's eastern margin and drains into Kuussuup Tasia (136 m asl) to the west, forming a long chain of connected basins. Tininnilik is dammed to the north by the GIS, and historic observations reveal that Tininnilik catastrophically drains beneath the ice margin every ca 7–10 years via the floating of the ice dam (Braithwaite and Thomsen, 1984; Weidick and Bennike, 2007; F. Nielsen, pers. comm., 2011). The filling and draining of the lake, characterized by a slow rise and rapid lowering of ca 65 m, likely relates to water depth and the buoyancy of the ice dam (Braithwaite and Thomsen, 1984; Furuya and Wahr, 2005). We conducted fieldwork in the QK and Tininnilik valleys in August 2010 after a draining event at Tininnilik that occurred between June 21 and July 7, 2010. Rock samples were collected for ^{10}Be exposure dating (hereafter termed ^{10}Be dating) from an island at the eastern side of Qinngap Ilulialeraa. Additionally, samples for radiocarbon dating were collected from a sediment core that was obtained from Kuussuup Tasia and from sediment exposures in both the Tininnilik and QK valleys.

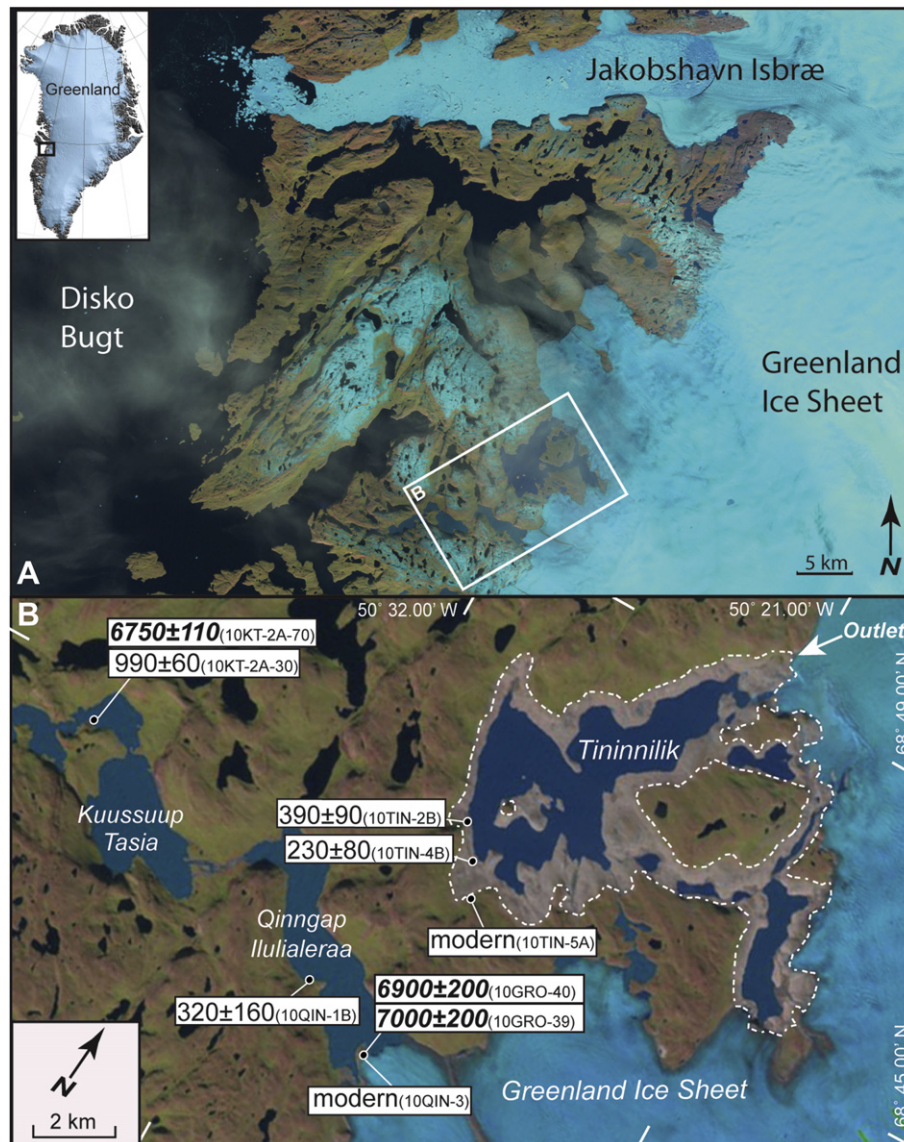


Fig. 1. (A) Composite Landsat image showing the position of the study area (white box) within southeastern Disko Bugt, with inset map (top left) showing the location of (A). Note Tininnilik is at a high-stand. (B) Landsat image of the study area (acquired on Aug. 17, 2010) showing ages (in cal yr BP) relating to early Holocene retreat (italicized bold text) and late Holocene advance (plain text) of the Greenland Ice Sheet margin. The dotted line denotes the high-stand shoreline for Tininnilik; the image was captured during a low-stand.

2.2. ^{10}Be dating

Two samples were collected for ^{10}Be dating on a small island that abuts the ice margin at the eastern side of Qinngap Ilulialeraa (Fig. 2). Samples 10GRO-40 (N 68°42.156', W 50°25.602'; 230 m asl) and 10GRO-41 (N 68°42.180', W 50°25.728'; 230 m asl) were collected from an erratic boulder and ice sculpted bedrock surface, respectively, using a hammer and chisel. We avoided the edges of sampled surfaces, and measured topographic shielding using a clinometer; sample sites had negligible topographic shielding. We recorded geographic coordinates and elevation with a handheld GPS device, estimated vertical error of ca 5 m. Samples underwent physical and chemical preparation at the University at Buffalo Cosmogenic Isotope Laboratory following procedures modified

from Kohl and Nishiizumi (1992). Samples were first crushed and sieved to isolate the 425–850 μm size fraction and then pretreated in dilute HCl and HNO_3 –HF acid baths. Quartz was isolated by heavy-liquid mineral separation followed by additional HNO_3 –HF treatment in heated sonication baths. ^9Be carrier (ca 0.4 g of 405 ppm) was added to each sample prior to dissolution in concentrated HF. Beryllium was extracted using ion-exchange chromatography, selectively precipitated with NH_4OH , and oxidized to BeO . $^{10}\text{Be}/^9\text{Be}$ AMS measurements were completed at the Lawrence Livermore National Laboratory, Center for Mass Spectrometry and normalized to the standard 07KNSTD3110 with a reported $^{10}\text{Be}/^9\text{Be}$ ratio of 2.85×10^{-12} (Nishiizumi et al., 2007, Table 1). The ratio for the dissolution process blank in the sample batch was 2.15×10^{-15} . ^{10}Be exposure ages were calculated using

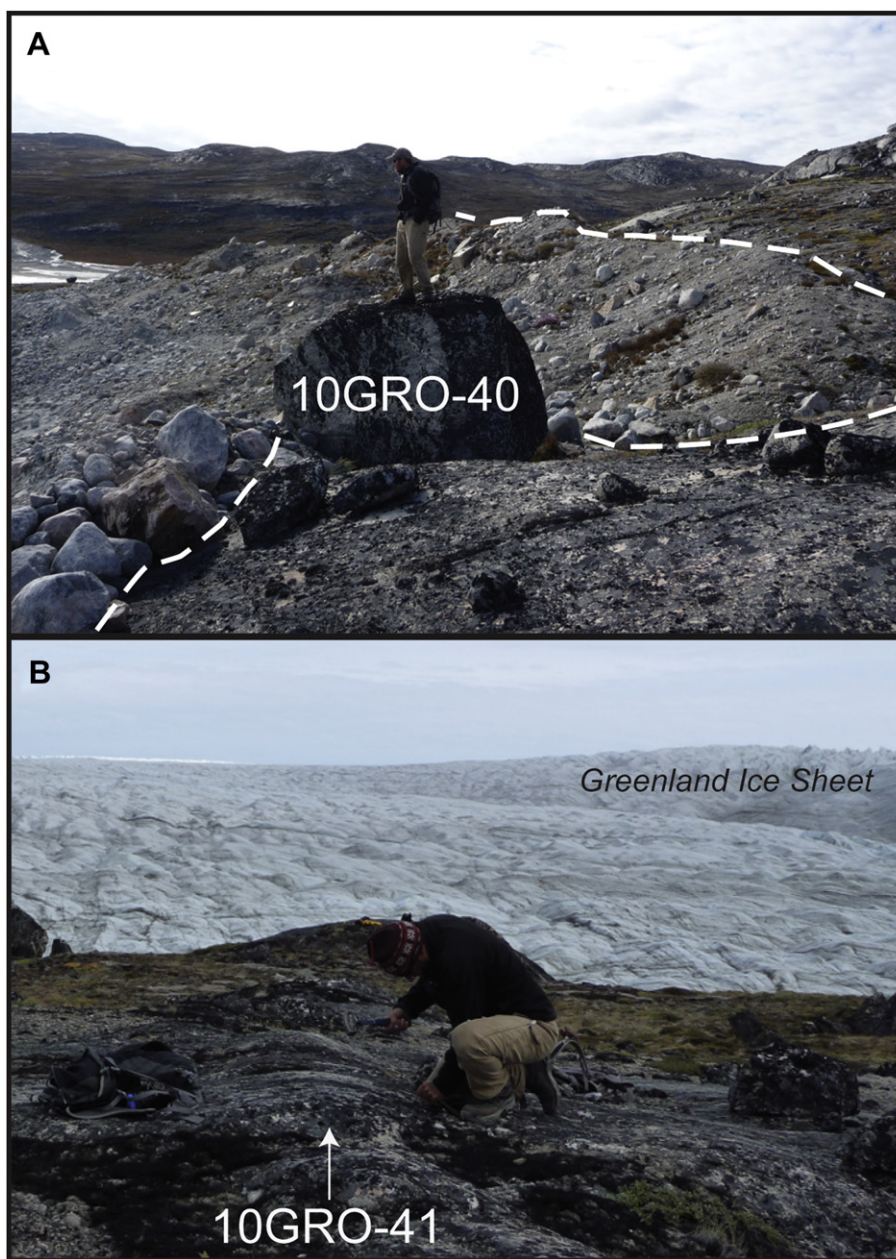


Fig. 2. Samples for ^{10}Be dating on the island at the eastern end of Qinngap Ilulialeraa. (A) Boulder located just outboard of historical moraine; note mature lichen cover on boulder and bedrock, but lack of lichen on boulders to the left, which were deposited between 1985 and 1997 AD; dotted line outlines the historical moraine. B. Bedrock surface located ca 25 m west (outboard) of the moraine shown in (A).

Table 1
¹⁰Be data for calculation of cosmogenic nuclide exposure ages.

Sample ID	Lat. (N)	Long. (W)	Elevation (m asl)	Sample height (m)	Thickness (cm)	Shielding correction	Quartz (g)	Be carrier added (g)	¹⁰ Be (atoms g ⁻¹)	¹⁰ Be uncertainty (atoms g ⁻¹)	¹⁰ Be age
36-10GRO-40	68.7026	-50.4267	230	2.5	1.0	1.0	50.1559	0.4006	37,757.0	868.4	6.9 ± 0.2
36-10GRO-41	68.7030	-50.4288	230	0.0	1.5	1.0	50.4674	0.4002	37,808.8	843.1	7.0 ± 0.2

¹⁰Be ages given in ka at 1SD using the scaling scheme of Lal (1991)/Stone (2000).

the CRONUS-Earth online calculator (<http://hess.ess.washington.edu/math>; Version 2.2; Balco et al., 2008) using the northeastern North America ¹⁰Be production rate (Balco et al., 2009) and the Lal/Stone scaling scheme (Lal, 1991; Stone, 2000); this production rate has been supported locally in western Greenland (Briner et al., 2012). Corrections due to the Earth's magnetic field are negligible as the samples are from high latitude (Gosse and Phillips, 2001). Corrections for snow cover were not made because sampled surfaces are from high points in the landscape and considered to be windswept of snow. Evidence of glacial abrasion on the bedrock surface indicates negligible post-glacial erosion.

2.3. Lake sediment coring

A 142-cm-long sediment core (10-KT-2A; N 68°43.875', W 50°41.127') was retrieved from a water depth of 26.13 m in Kuusuup Tasia. The core was collected using a piston coring system operated from a floating cataraft platform. Lake bathymetry was measured using a Garmin GPSMAP 400 series GPS receiver connected to a dual beam depth transducer. The sediment core was transported to the University at Buffalo, where magnetic susceptibility was measured every 5 mm using a Barrington MS2E High Resolution Surface Scanning Sensor scanner connected to a Barrington MS2 Magnetic Susceptibility meter. Organic matter content was measured every 5 mm using a loss-on-ignition procedure, with heating at 550 °C. The core was sampled at two locations for radiocarbon dating; a sample (10-KT-2A-70) of aquatic plant matter was picked from 70 cm depth and a bulk sediment sample (10-KT-2A-30) was collected from 30 cm depth.

2.4. Radiocarbon dating

Seven samples were collected for radiocarbon dating; two samples were extracted from core 10-KT-2A, and the remaining samples were collected from sediment exposures in the field (Table 2). All samples were transported to the University at Buffalo where they underwent washing with deionized water; the bulk

sediment sample was freeze-dried. Radiocarbon ages from the National Ocean Sciences Accelerator Mass Spectrometry Facility at Woods Hole Oceanographic Institution were calibrated using the CALIB v 6.0 (Stuiver et al., 2010) and the IntCal09 calibration curve (Reimer et al., 2009, Table 2). Two “modern” values were converted to calendar years using the CALIBomb program (<http://calib.qub.ac.uk/CALIBomb/>; Reimer et al., 2009) with the NH_zone1 dataset compilation (Hua and Barbetti, 2004, Table 2). All calibrated radiocarbon ages are reported in the manuscript as the midpoint ± half of the 2σ age range.

2.5. Remote sensing

To document the spatial variability of ice-margin change over the 20th century, we measured ice-margin retreat throughout western Greenland. We digitized the boundary between fully vegetated landscapes and those lacking vegetation cover for the area abutting the ice sheet from 61.10° N to 73.84° N. In most locations, this boundary is a moraine, locally termed the historical moraine, which has been correlated with the LIA (Weidick, 1968; Kelly and Lowell, 2009). In some locations the boundary is expressed simply as a vegetation trimline. We measured the distance between the historic moraine/trimline and the present ice margin as depicted in the most recent clear GeoEye, and Landsat imagery. This imagery was captured using the GeoEye-1, OrbView, IKONOS, QuickBird, WorldView, Landsat 5 and Landsat 7 satellites between 2002 and 2011 AD. This compilation had a maximum resolution of 30 m; some imagery has a resolution of 2 m. Measurements of retreat distance were made parallel to the direction of ice flow at every 5 km along the ice margin throughout western Greenland. In locations where large outlet glaciers extend from the ice sheet, measurements were taken at the lobe terminus in 5 km increments only, rather than down the sides of the lobe. The measurements were sorted into marine- ($n = 66$) and land-terminating ($n = 311$) glaciers, with all glaciers not terminating in marine water classified as “land terminating.” A second distinction identified the largest outlet glaciers ($n = 6$), these are: Upernavik

Table 2
 Radiocarbon ages and associated sample information.

Core/site	Depth (cm)	Lat. (N)	Long. (W)	Lab number	Material dated	Fraction modern	δ ¹³ C (‰PDB)	Radiocarbon age (¹⁴ C yr BP)	Calibrated age ranges BP (2σ)	Cal. years BP
Pre-modern										
10TIN-2B	2	68 45.497'	50 27.52'	OS-85086	Plant/wood	0.9613 ± 0.0044	-27.54	320 ± 40	300–470	390 ± 90
10TIN-4B	6	68 45.175'	50 26.128'	OS-85085	Plant/wood	0.9737 ± 0.0035	-27.89	220 ± 30	0–20, 150–220, 270–310	230 ± 80
10QIN-1B	35	68 42.675'	50 28.498'	OS-85119	Plant/wood	0.9643 ± 0.0055	-25.26	290 ± 50	150–180, 280–480	320 ± 160
10KT-2A-30	30–30.5	68 43.875'	50 41.127'	OS-85023	Bulk sediment	0.876 ± 0.0030	-21.83	1060 ± 30	930–1000, 1030–1050	990 ± 60
10KT-2A-70	69.5–70	68 43.875'	50 41.127'	OS-85357	Plant matter	0.47953 ± 0.0025	-30.42	5900 ± 40	6640–6850	6750 ± 110
Modern dates										
Years A.D.										
10TIN-5A	0	68 44.900'	50 25.284'	OS-85080	Plant/wood	1.2146 ± 0.0040	-26.76	Modern	1959–1961 or 1983–1985	na
10QIN-3	0	68 42.626'	50 28.400'	OS-85079	Plant/wood	1.2723 ± 0.0040	-28.08	Modern	1959, 1962, 1979–1981	na

Note: Calibrated ages are rounded to the nearest decade.

Isstrøm, Jakobshavn Isbræ, Akugdlerssup Sermia, Kangiata Nunata Sermia, Eqalorutsit Kitdlit Sermiat, and Qajuuttap Sermia.

3. Results and interpretation

3.1. Qinngap Ilulialeraa–Kuussuup Tasia valley

The two samples for ^{10}Be dating that we collected from the small island at the eastern end of Qinngap Ilulialeraa (Fig. 2) from ice-sculpted bedrock (10GRO-40) and an erratic boulder perched on bedrock (10GRO-41) are 6900 ± 200 and 7000 ± 200 yr BP, respectively (Fig. 1; Fig. 2; Table 1). Both samples lie outboard of a fresh-appearing moraine that delineates a boundary between a vegetated landscape and one devoid of vegetation. Thus, the ages provide a direct constraint on the timing of post-Last Glacial Maximum deglaciation in the QK valley.

The sediment core from Kuussuup Tasia contains three primary units, defined by visual stratigraphy, magnetic susceptibility and organic-matter content (Fig. 3). The bottom unit is a gray minerogenic-rich unit (0.72 m thick) defined by low organic-matter content and high magnetic susceptibility values. The middle unit is a gray-brown organic-rich unit (0.4 m thick) defined by high organic-matter content and low magnetic susceptibility values. The upper unit is a gray minerogenic-rich unit (0.3 m thick) with low organic-matter content and high magnetic susceptibility values. The alternating units of organic- and minerogenic-rich sediment with sharp contacts are typical of proglacial-threshold lakes, and

reflect periods of time when the ice margin terminated in (minerogenic-rich sediments), or out of (organic-rich sediments) the lake's drainage basin (Briner et al., 2010). A radiocarbon age of 6750 ± 110 cal yr BP (10-KT-2A-70) from just above the lower contact between minerogenic- and organic-rich sediments constrains the timing of ice retreat out of the catchment (Fig. 1; Table 2). A second radiocarbon age from the core, extracted just below the upper contact between organic rich-sediment and overlying minerogenic-rich sediment of 990 ± 60 cal yr BP (10-KT-2A-30) suggests that ice advanced back into the lake catchment shortly after this time (Fig. 1; Fig. 3; Table 2). However, we treat this age with caution and consider it a maximum limiting age, because it is derived from bulk sediments. It has been noted in a number of studies that bulk sediment may give erroneously old ages in comparison to macrofossil-based ages by 100–400 years in western Greenland (Kaplan et al., 2002; Bennike et al., 2010).

The late Holocene advance of the GIS margin in the QK valley may also be recorded in a sediment sequence exposed ca 2 km west of the current ice margin. The 0.95-m-tall sediment section exposed on the southern shore of Qinngap Ilulialeraa comprises peat-rich sediments overlain by eolian sand (Fig. 4). We interpret this stratigraphy to reflect a shift from a stable and fully-vegetated landscape to one with locations of sand mobilization, which records the approaching ice margin and associated increase in frequency and strength of katabatic wind (e.g., Willemse et al., 2003). A sample (10QIN-1B) from the uppermost peat layer yields a radiocarbon age of 320 ± 160 cal yr BP, suggesting that the ice margin may have neared its current position at or shortly after this time (Fig. 1; Table 2).

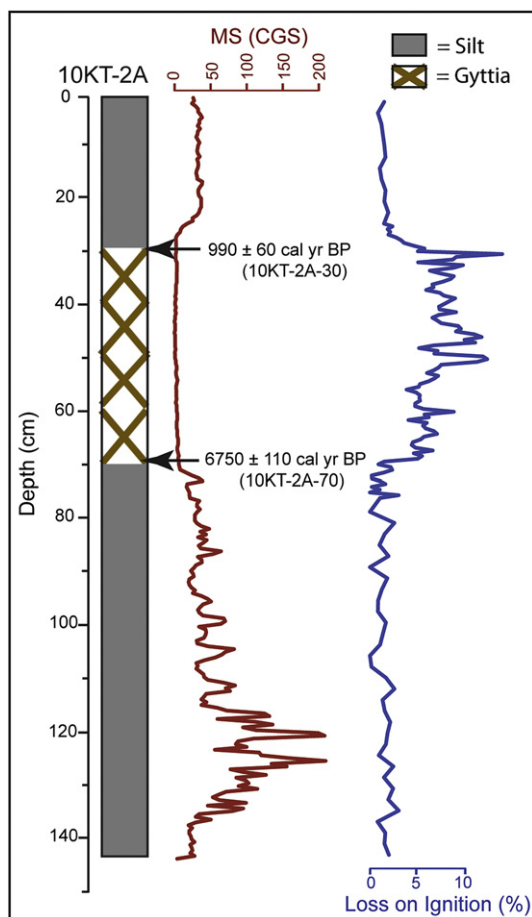


Fig. 3. Stratigraphy and downcore data of lake sediment core 10KT-2A, with solid gray pattern representing minerogenic-rich sediment and the crosshatch pattern representing organic-rich sediment.

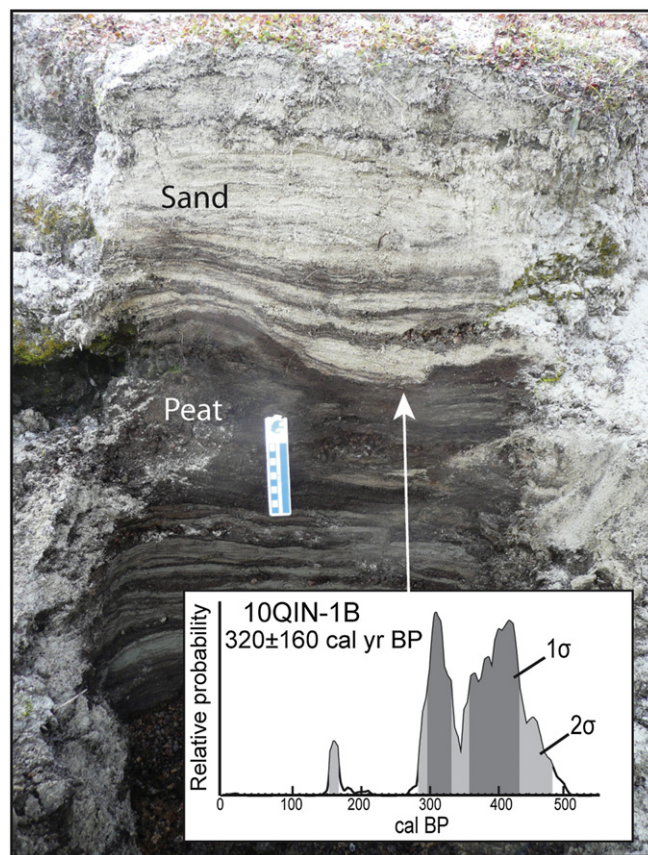


Fig. 4. Stratigraphic section exposing peat-rich sediments overlain by sand-rich sediments. The arrow shows the location of sample 10QIN-1B. Inset shows radiocarbon calibration of 10QIN-1B.

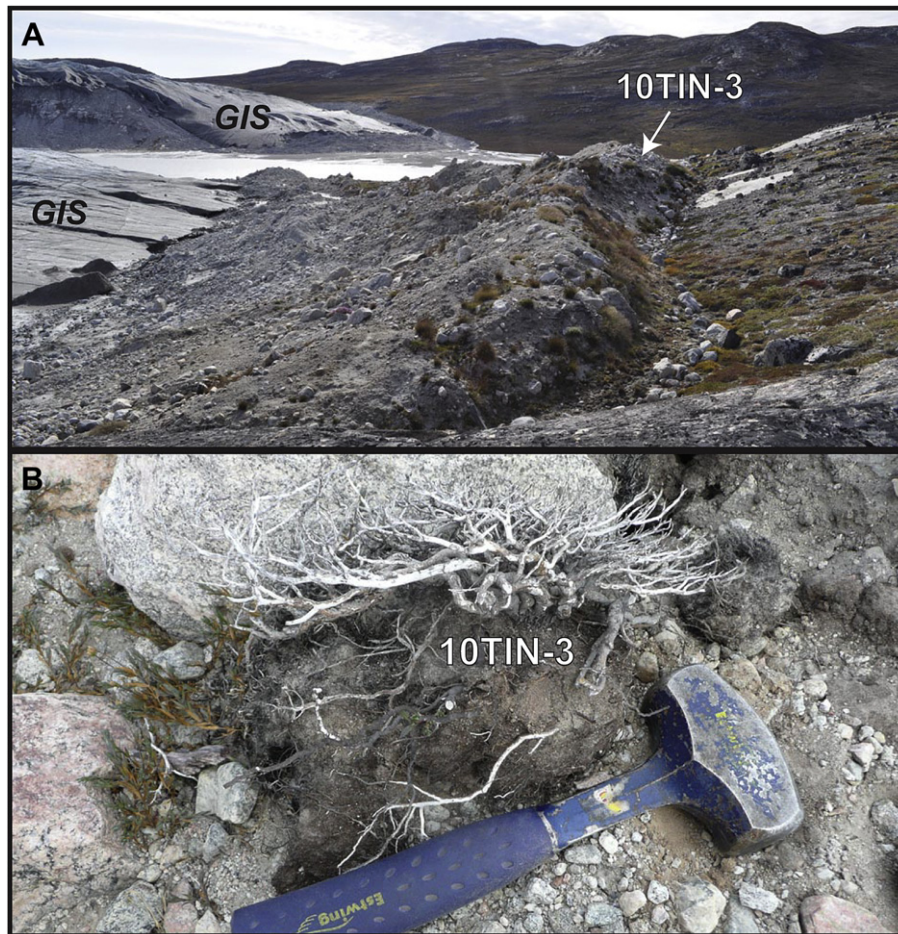


Fig. 5. (A) View to the south of the historical moraine (1985–1997 AD) on the island at the eastern end of Qinngap Ilulialeraa, with the current ice margin on the left side of the photo. The arrow indicates the location where sample 10TIN-3 was collected. (B) A close-up photograph of 10TIN-3.

To determine the timing of maximum late Holocene ice extent, we collected *Betula* samples from a rooted tundra mat (10QIN-3; Fig. 5) that had been overrun and incorporated into the moraine on the island at the eastern end of Qinngap Ilulialeraa (Fig. 6). A sample from the outermost growth rings yielded a post-bomb radiocarbon age with solutions of 1959–1962 and 1979–1985 AD (Table 2). Aerial photographs of the ice margin acquired in 1949, 1953 and 1985 AD reveal ice advance through this time period, although not yet reaching the island (Fig. 6). A ground-based photograph taken of the island at the head of Qinngap Ilulialeraa in 1997 AD shows that the ice had reached the island and the moraine had been formed by that time (F. Nielsen, pers. comm., 2011). Combined, the maximum-limiting radiocarbon age and the photographs constrain deposition of the moraine to be between 1985 and 1997 AD.

3.2. Tininnilik valley

We derived additional chronologic constraints for the late Holocene advance of the GIS from the Tininnilik valley (Fig. 1). The partial draining of Tininnilik prior to our visit exposed much of the lake bottom. A 0.7-m-tall sediment section, exposed by iceberg scour, comprises till overlain by alternating peat-rich sediments and soil horizons, which are in turn overlain by a thin layer of inorganic glaciolacustrine sediment (Fig. 7). The sediment sequence is interpreted to represent early Holocene deglaciation, followed by ice- and lake-free conditions during the middle Holocene, followed by glaciolacustrine deposition when the advancing

GIS dammed the Tininnilik valley. A plant fragment (10TIN-2B) in growth position buried by glaciolacustrine sediments yielded a radiocarbon age of 390 ± 90 cal yr BP (Fig. 1; Table 2). A second stratigraphic section, 1.0 m tall and lower in the lake basin, contains peat-rich sediments overlain by cross-bedded inorganic sands; we interpret the sand to have been deposited during a lake low-stand by a prograding delta after the lake originally formed (Fig. 7). The uppermost plant material beneath the sand yielded a radiocarbon age of 150 ± 150 cal yr BP (Fig. 1; Table 2); after excluding an age solution of 9 ± 10 cal yr BP that is inconsistent with historic observations of Tininnilik's existence, the radiocarbon age becomes 230 ± 80 cal yr BP. Thus, evidence from Tininnilik suggests that the ice margin advanced or thickened enough to dam the Tininnilik valley after 230 ± 80 cal yr BP.

Tininnilik's maximum high-stand is marked by a subtle shoreline and a wave-washed zone littered with dead shrubs; rocky surfaces in the washed zone and below are devoid of lichen, likely due to periodic inundation. The outermost growth rings from a dead *Salix* shrub (10TIN-5A; Fig. 8) within the wave-washed zone yielded a post-bomb radiocarbon age with solutions of 1959–1961 AD and 1983–1985 AD (Table 2). If the maximum high-stand of Tininnilik corresponds with the maximum thickness of the ice dam, then this supports a mid- to late-20th century timing of late Holocene maximum ice extent. Alternatively, the maximum high-stand might relate to other factors involving the re-configuration of the subglacial conduit system at the outflow. However, because the age of the Tininnilik high-stand is coeval with the age of

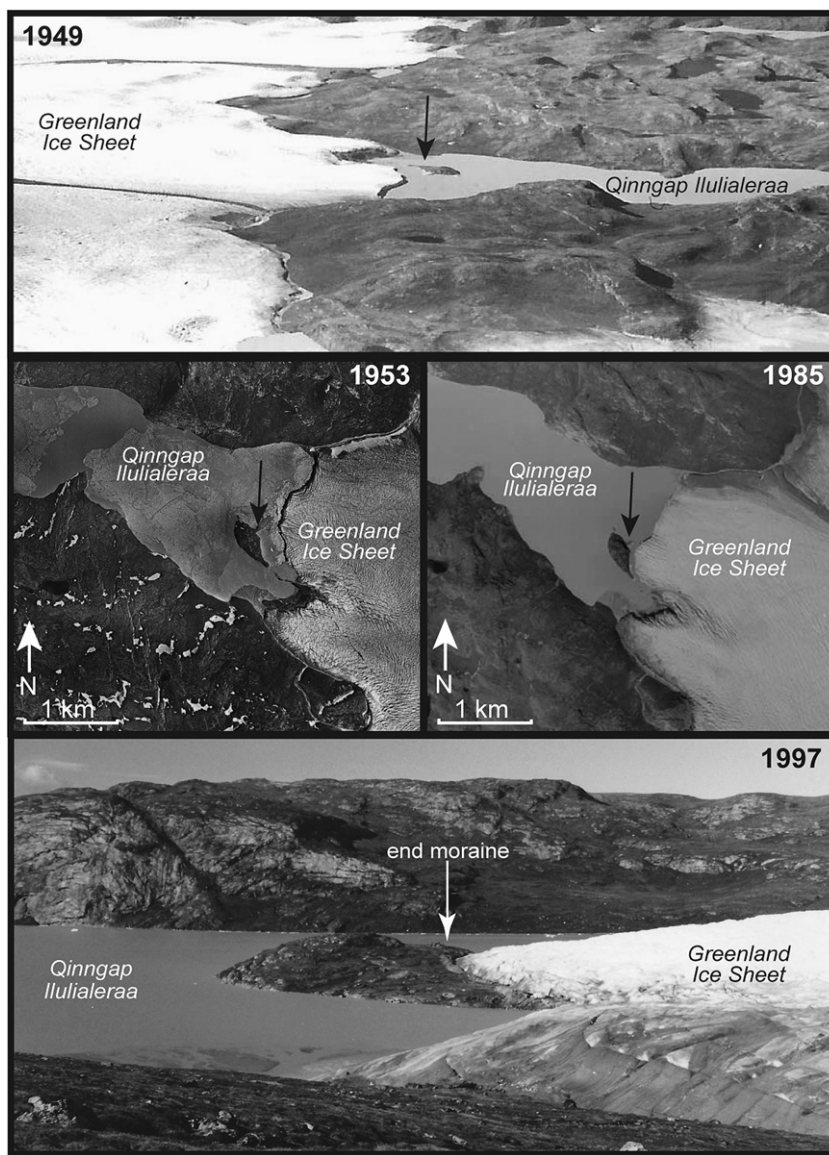


Fig. 6. Historical images of the Greenland Ice Sheet margin at Qinngap Ilulialeraa. Note that the ice margin lies east of the island in the oblique aerial photo from 1949 AD (view to the south) and in the vertical aerial photographs from 1953 and 1985 AD. The ice margin rested on the island, and a small moraine had formed, by 1997 AD (view to the north; photograph courtesy of Frank Nielsen). The arrow indicates the position of the maximum late Holocene ice limit in all photographs.

maximum ice extent at the head of Qinngap Ilulialeraa, we favor the interpretation that the high-stand relates to maximum ice thickness at the ice dam.

3.3. Spatial variability of ice-margin change

Our survey of ice-margin retreat in western Greenland reveals large-scale frontal retreat of marine-terminating outlet glaciers throughout the 20th century (average retreat = 3820 m; median retreat = 535 m), which exhibited one to two orders of magnitude greater retreat than adjacent land-terminating sectors (average retreat = 340 m; median retreat = 0 m; Fig. 9). Even after excluding the six largest marine-terminating glaciers, the remaining marine glaciers still exhibit significantly more retreat (average retreat = 1210 m; median retreat = 400 m) than land-terminating ice margin sectors. This dichotomy clearly illustrates a significant difference in behavior between marine- and land-terminating ice margins in the 20th century (Fig. 9).

A second notable feature of our compilation is the prevalence of sections of the ice margin that display negligible retreat (Fig. 9), which has been previously recognized in some specific ice-margin locations (Warren and Glasser, 1992; Weidick, 1994, 2009; Knight et al., 2000). However, more surprising, is the lack of a distinct vegetation trimline or an unvegetated moraine, locally recognized as the 'historical moraine' (Weidick, 1968), fronting vast stretches of the ice margin. For example, our analysis reveals that ca 54% of the surveyed ice margin (ca 89% of which are land-terminating sectors) demonstrated <50 m of net retreat during the 20th century (Fig. 9). This suggests either negligible post-LIA net retreat, or a net advance beyond the LIA ice-margin position during the 20th century, similar to the ice-margin histories in Tininnilik and QK valleys.

4. Discussion

We show that our field site deglaciated ca 7000 years BP, which was followed by advancing ice during the late Holocene that

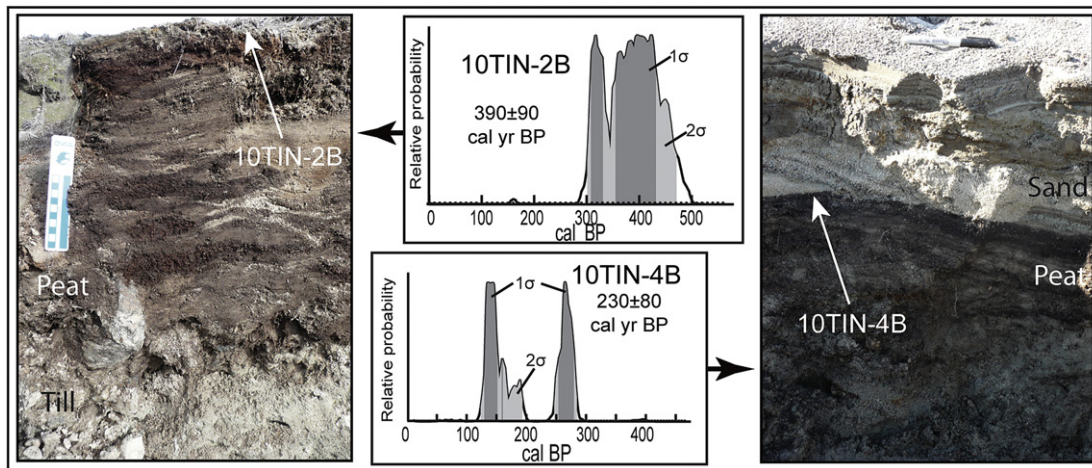


Fig. 7. Sediment exposures from the Tininnilik basin. Photo at left shows a 70-cm-tall-exposure comprising till overlain by peat overlain by a thin coating of lacustrine silt; sample location for 10TIN-2B shown with arrow. Photo at right shows a 1-m-tall exposure comprising peat overlain by stratified sand. Sample location for 10TIN-4B shown with arrow; note marker at top for scale. Plots show radiocarbon age calibrations.

culminated in the late 20th century, when the ice margin was more extensive than during the LIA. These results reveal a pattern of ice-margin change during the late Holocene that differs from marine-terminating glaciers in western Greenland and most other glaciers worldwide (e.g., Lowell, 2000; Oerlemans, 2005). Furthermore, based on our broader survey, it appears that this unusual ice-margin history is not isolated to these valleys, but occurred at many locations throughout western Greenland, where negligible retreat has occurred since the LIA. Although time periods with glacier advance during the late 20th century are not unique, the fact that ice was more extensive during the late 20th century than any other time in the late Holocene is remarkable for such large sectors of an ice sheet.

The spatial complexity of ice-margin change is exemplified by the disparity in the behavior of neighboring sectors of the ice margin, which is likely due to a variety of factors. Although our analysis did not quantify average thinning rates, we note that on the spatial and temporal scales involved in this study, frontal retreat and thinning occur together. Indeed, Kjær et al. (2012) revealed high correlation between frontal retreat and thinning for the ice-sheet margin throughout northwest Greenland. Thus, we suggest that our analysis of frontal retreat is an appropriate proxy for overall ice margin behavior. In any case, we doubt that our reconstructed spatial pattern of ice-margin change can be solely

explained by variable trends in climate given the proximity in which significant differences in ice-margin change occurred (Sole et al., 2008). Rather, the contrasting behavior probably lies in the variety of ice-dynamical processes that are unique to marine-terminating glaciers. In addition to being affected by changes in surface mass balance, marine-terminating glacier termini are influenced by changes at their calving fronts (Pfeffer, 2007; Nick et al., 2009). Oceanographic conditions can act as a major influence on the behavior of marine-terminating glaciers through submarine melting and destabilization of the calving front (e.g., Holland et al., 2008; Rignot et al., 2010). Combined, these factors can lead to larger magnitude responses at marine- versus land-terminating glaciers. Our survey of ice-margin change in western Greenland supports this concept: marine-terminating glaciers retreated significantly more throughout the 20th century than their land-terminating counterparts.

An additional important difference between marine- and land-terminating sectors of the GIS is surface velocity. The surface velocity of marine-terminating glaciers is typically one to two orders of magnitude greater than land-terminating glaciers (Joughin et al., 2010). Surface velocity is linked to glacier response time, such that faster-flowing ice can respond more quickly to a climate perturbation and vice versa (Bamber et al., 2007). We suggest that short response time may help explain the seemingly close connection with climate displayed by marine-terminating glaciers (Lloyd et al., 2011; Young et al., 2011b), and longer response time would explain the lack of correlation with climate displayed by many land-terminating glaciers in western Greenland. Weidick (1994) suggested that the response time of some GIS land-terminating glaciers is on the order of centuries. Thus, it is possible that due to a long response time, the GIS margin in the QK and Tininnilik valleys advanced during the 20th century as a response to prior cooling, such as during the LIA, and has yet to demonstrate frontal retreat in response to the cumulative negative surface mass balance that has occurred since the LIA. Furthermore, a lagged response of land-terminating ice margin sectors to prior cooling is supported by surface mass balance data. Using an ice sheet mass balance model forced by 19th and 20th century instrumental data, Wake et al. (2009) predict that there should have been tens to hundreds of meters of thinning from 1866 to 2005 AD in western Greenland. This is in contrast to our observations of negligible retreat in many areas, implying that vast stretches of the south-western GIS are not in equilibrium with 20th century climate



Fig. 8. Photograph of maximum high-stand shoreline along the southern margin of Tininnilik, with an arrow indicating the location where sample 10TIN-5A was collected. Note stranded iceberg in the center of the photo, and silt cover on the landscape in the foreground, both indicative of recent (1 month prior to photo) draining event.

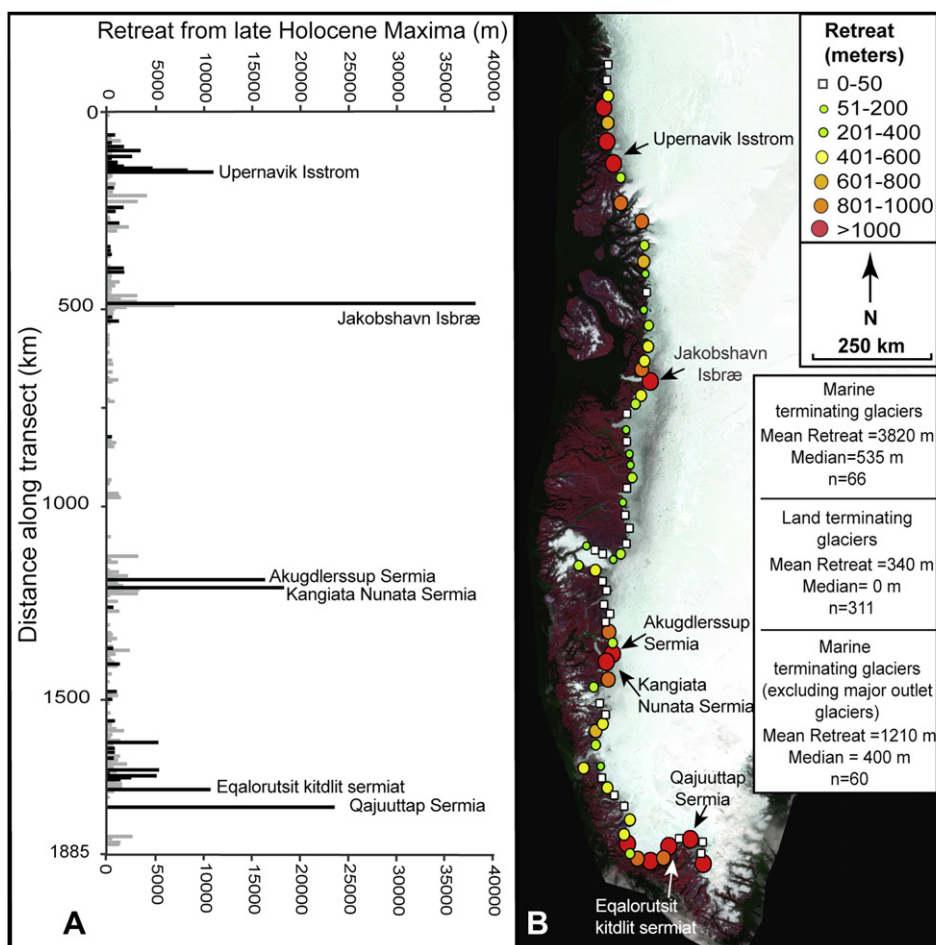


Fig. 9. (A) Ice-margin retreat measured in western Greenland plotted as distance from the northern end of the survey; large outlet glaciers are labeled; gray bars denote retreat of land-terminating ice margin, black bars denote retreat of marine-terminating ice margins. (B) MODIS image of western Greenland showing average ice-margin retreat from the late Holocene maximum to the 2000s AD. Symbols indicate average retreat over a 25-km-long segment of ice margin, each comprised of 5 individual measurements spaced every 5 km. This figure is available in color online at <http://www.journals.elsevier.com/quaternary-science-reviews/>.

change. Thus, we suggest that ice-sheet response time, in addition to dynamic factors that exacerbate the response of marine glaciers to climate change, can explain the contrasting histories of land- and marine-terminating glaciers in western Greenland.

5. Conclusion

Our results demonstrate that two land-terminating sectors of the southwestern GIS attained their late Holocene maximum positions during the late 20th century, and so far have not been significantly impacted by post-LIA warming. Furthermore, the response of the GIS to recent climate change has not been uniform. Rather, there is significant variability in the timing and magnitude of ice-margin change across western Greenland during the last few centuries. Out-of-phase timing of ice-margin change between adjacent land- and marine-terminating glaciers over the 20th century indicates that land-terminating ice margins in western Greenland do not respond quickly (i.e., within decades) to climate change (cf. Bjork et al., 2012). Rather, heterogeneous ice-margin response is likely due to the complex interplay among several variables, including dynamical processes associated with calving termini and ice-sheet response time. Variability in response time implies that much of the GIS margin, particularly low-velocity land-terminating glaciers, is not in equilibrium with climate at present. This leaves open the

possibility for accelerated retreat of land-terminating ice margins in the near future as these regions respond to 20th and 21st century warming.

Acknowledgments

We thank Stefan Truex and Elizabeth Thomas for assistance with fieldwork, Shana Losee and Sarah Lavin for invaluable help in the laboratory, CH2M Hill Polar Field Services for help with field logistics, the 109th Air National Guard for transportation to and from Greenland, and Kurt Kjær at the University of Copenhagen for aerial photographs, and Frank Nielsen for sharing knowledge and photographs of the field area. We thank Michael Kaplan, Elizabeth Thomas and two anonymous reviewers whose comments improved this manuscript. This research was supported by NSF-ARC-0909334 and NSF-BCS 0752848/1002597 to JPB, and NNX10AV13G and NNX10AO66H to BC.

References

- Balco, G., Stone, J.O., Lifton, N.A., 2008. A complete and easily accessible means of calculating surface exposure ages or erosion rates from ^{10}Be and ^{26}Al measurements. *Quaternary Geochronology* 3, 174–195.
- Balco, J.G., Briner, J.P., Finkel, R.C., 2009. Regional beryllium-10 production rate calibration for northeastern North America. *Quaternary Geochronology* 4, 93–107.

- Bamber, J.L., Alley, R.B., Joughin, I., 2007. Rapid response of modern day ice sheets to external forcing. *Earth and Planetary Science Letters* 257, 1–13.
- Bennike, O., Anderson, N.J., McGowan, S., 2010. Holocene palaeoecology of south-west Greenland inferred from macrofossils in sediments of an oligosaline lake. *Journal of Paleolimnology* 43, 787–798.
- Bjork, A.A., Kjær, K.F., Korsgaard, N.J., Khan, S.A., Kjeldsen, K.K., Andresen, C.S., Box, J.E., Larsen, N.K., Funder, S., 2012. An aerial view of 80 years of climate-related glacier fluctuations in southeast Greenland. *Nature Geoscience* 5, 427–432.
- Braithwaite, R.J., Thomsen, H.H., 1984. Runoff conditions at Paakitusp Akuliarusersua, Jakobshavn, estimated by modeling. *Grønlands Geologiske Undersøgelse Gletscher-hydrologiske Meddelelser* 84/3, 22.
- Briner, J.P., Young, N.E., Goehring, B.M., Schaefer, J.M., 2012. Constraining ^{10}Be production rates on Greenland. *Journal of Quaternary Science* 27, 1–5.
- Briner, J.P., Young, N.E., Thomas, E.K., Stewart, H.A.M., Losee, S., Truex, S., 2011. Varve and radiocarbon dating support the rapid advance of Jakobshavn Isbræ during the Little Ice Age. *Quaternary Science Review* 30, 2476–2486.
- Briner, J.P., Stewart, H.A.M., Young, N.E., Philips, W., Losee, S., 2010. Using proglacial-threshold lakes to constrain fluctuations of the Jakobshavn Isbrae ice margin, western Greenland, during the Holocene. *Quaternary Science Reviews* 29, 3861–3874.
- Csatho, B., Schenk, T., van der Veen, C.J., Krabill, W.B., 2008. Intermittent thinning of Jakobshavn Isbræ, West Greenland, since the Little Ice Age. *Journal of Glaciology* 54, 131–144.
- Furuya, M., Wahr, J.M., 2005. Water level changes at an ice-dammed lake in west Greenland inferred from InSAR data. *Geophysical Research Letters* 32, L14501.
- Gosse, J.C., Phillips, F.M., 2001. Terrestrial *in situ* cosmogenic nuclides: theory and application. *Quaternary Science Reviews* 20, 1475–1560.
- Holland, D.M., Thomas, R.H., Young, B.D., 2008. Acceleration of Jakobshavn Isbræ triggered by warm subsurface ocean waters. *Nature Geoscience* 1, 659–664.
- Hua, Q., Barbetti, M., 2004. Review of tropospheric bomb radiocarbon data for carbon cycle modeling and age calibration purposes. *Radiocarbon* 46, 1273–1298.
- Joughin, I., Abdalati, W., Fahnestock, M., 2004. Large fluctuations in speed on Greenland's Jakobshavn Isbræ glacier. *Nature* 432, 608–610.
- Joughin, I., Smith, B.E., Howat, I.M., 2010. Greenland flow variability from ice-sheet-wide velocity mapping. *Journal of Glaciology* 56, 415–430.
- Kaplan, M.R., Wolfe, A.P., Miller, G.H., 2002. Holocene environmental variability in southern Greenland inferred from lake sediments. *Quaternary Research* 58, 149–159.
- Kelly, M.A., Lowell, T.V., 2009. Fluctuations of local glaciers in Greenland during the latest Pleistocene and Holocene time. *Quaternary Science Reviews* 28, 2088–2106.
- Kjær, K.H., Khan, S.A., Korsgaard, N.J., Wahr, J., Bamber, J.L., Hurkmans, R., van den Broeke, M., Timm, L.H., Kjeldsen, K.K., Björk, A.A., Larsen, N.K., Jørgensen, L.T., Færch-Jensen, A., Willerslev, E., 2012. Aerial photographs reveal late-20th-century dynamic ice loss in Northwestern Greenland. *Science* 337, 569–573.
- Knight, P.G., Walier, R.I., Paterson, C.J., 2000. Glacier advance, ice-marginal lakes and routing of meltwater and sediment: Russell Glacier, Greenland. *Journal of Glaciology* 46, 423–426.
- Kohl, C.P., Nishiizumi, K., 1992. Chemical isolation of quartz for measurement of *in situ*-produced cosmogenic nuclides. *Geochimica et Cosmochimica Acta* 56, 3583–3587.
- Lal, D., 1991. Cosmic ray labeling of erosion surfaces: *in situ* nuclide production rates and erosion models. *Earth and Planetary Science Letters* 104, 424–439.
- Lloyd, J., Moros, M., Perner, K., Telford, R.J., Kuipers, A., Jansen, E., McCarthy, D., 2011. A 100 yr record of ocean temperature control on the stability of Jakobshavn Isbrae, West Greenland. *Geology* 39, 867–870.
- Long, A.J., Woodroffe, S.A., Roberts, D.H., Dawson, S., 2011. Isolation basins, sea-level changes and the Holocene history of the Greenland Ice Sheet. *Quaternary Science Reviews* 30, 3748–3768.
- Lowell, T.V., 2000. As climate changes, so do glaciers. *Proceedings of the National Academy of Sciences of the United States of America* 97, 1351–1354.
- Nick, F.M., Vieli, A., Howat, I.M., Joughin, I., 2009. Large-scale changes in Greenland outlet glacier dynamics triggered at the terminus. *Nature Geoscience* 2, 110–114.
- Nishiizumi, K., Imamura, M., Caffee, M., Southon, J., Finkel, R., McAnich, J., 2007. Absolute calibration of ^{10}Be AMS standards. *Nuclear Instruments and Methods in Physics Research* 258, 403–413.
- Oerlemans, J., 2005. Extracting a climate signal from 169 glacial records. *Science* 308, 675–677.
- Pfeffer, W.T., 2007. A simple mechanism for irreversible tidewater glacier retreat. *Journal of Geophysical Research* 112, F03S25.
- Porter, S.C., 2007. Glaciations: Neoglaciation in the American Cordilleras: Encyclopedia of Quaternary Science. Elsevier Inc., pp. 1133–1142.
- Reimer, P.J., Baillie, M.G.L., Bard, E., Bayliss, A., Beck, J.W., Blackwell, P.G., Bronk, Ramsey, C., Buck, C.E., Burr, G.S., Edwards, R.L., Friedrich, M., Grootes, P.M., Guilderson, T.M., Hajdas, I., Heaton, T.J., Hogg, A.G., Hughen, K.A., Kaiser, K.F., Kromer, B., McCormac, F.G., Manning, S.W., Reimer, R.W., Richards, D.A., Southon, J.R., Talamo, S., Turney, C.S.M., van der Plicht, J., Weyhenmeyer, C.E., 2009. IntCal09 and Marine09 Radiocarbon Age Calibration. *Journal of Geophysical Research* 114, F03S25.
- Rignot, E., Kanagaratnam, P., 2006. Changes in the velocity structure of the Greenland ice sheet. *Science* 311, 986–990.
- Rignot, E., Box, J.E., Burgess, E., Hanna, E., 2008. Mass balance of the Greenland Ice Sheet 1958 to 2007. *Geophysical Research Letters* 35, L20502.
- Rignot, E., Koppes, M., Velicogna, I., 2010. Rapid submarine melting of the calving faces of west Greenland glaciers. *Nature Geoscience* 3, 187–191.
- Sole, A., Payne, T., Bamber, J., Nienow, P., Krabill, W., 2008. Testing hypotheses of the cause and peripheral thinning of the Greenland Ice Sheet: is land-terminating ice thinning at anomalously high rates? *The Cryosphere* 2, 205–218.
- Stone, J.O., 2000. Air pressure and cosmogenic isotope production. *Journal of Geophysical Research* 105, 23753–23759.
- Stuiver, M., Reimer, P.J., Reimer, R.W., 2010. CALIB 6.0. WWW program and documentation available at: <http://calib.qub.ac.uk/calib/>.
- Van den Broeke, M., Bamber, J., Ettema, J., Rignot, E., Schrama, E., Van de Bern, W.J., Van Meijgaard, E., Velicogna, I., Wouters, B., 2009. Partitioning recent Greenland mass loss. *Science* 326, 984–986.
- Wake, L.M., Huybrechts, P., Box, J.E., Hanna, E., Janssens, I., Milne, G.A., 2009. Surface mass-balance changes of the Greenland ice sheet since 1866. *Annals of Glaciology* 50, 178–184.
- Warren, C.R., Glasser, N.F., 1992. Contrasting response of South Greenland Glaciers to recent climatic change. *Arctic, Antarctic, and Alpine Research* 24, 124–132.
- Weidick, A.W., 1968. Observations on some Holocene glacier fluctuations in west Greenland. *Meddelelser Om Grønland* 165, 202.
- Weidick, A., 1992. Jakobshavn Isbræ area during the climatic optimum. *Rapport Grønlands Geologiske Undersøgelse* 155, 67–72.
- Weidick, A.W., 1994. Historical fluctuations of calving glaciers in South and West Greenland. *Rapport Grønlands Geologi Unders* 161, 73–79.
- Weidick, A.W., 2009. Johan Dahl Land, south Greenland: the end of 20th century glacier expansion. *Polar Record* 45, 337–350.
- Weidick, A., Bennike, O., 2007. Quaternary glaciation history and glaciology of Jakobshavn Isbræ and the Disko Bugt region, west Greenland: a review. *Geological Survey of Denmark and Greenland Bulletin* 14, 78.
- Willemse, N.W., Koster, E.A., Hoogakker, B., Van Tatenhove, F.G.M., 2003. A continuous record of Holocene eolian activity in West Greenland. *Quaternary Research* 59, 322–334.
- Young, N.E., Briner, J.P., Stewart, H.A.M., Axford, Y., Csatho, B., Rood, D.H., Finkel, R.C., 2011a. Response of Jakobshavn Isbræ, Greenland, to Holocene climate change. *Geology* 39, 131–134.
- Young, N.E., Briner, J.P., Axford, Y., Csatho, B., Babonis, G.S., Rood, D.H., Finkel, R.C., 2011b. Response of a marine-terminating Greenland outlet glacier to abrupt cooling 8200 and 9300 years ago. *Geophysical Research Letters* 38, L24701.